

## CHAPTER III



## ELABORATED MODEL OF PHOTOCURRENT IN N-ON-P JUNCTION SOLAR CELLS

3.1 Introduction

Numerical simulation of photocurrent is carried out in each regions of n-on-p silicon solar cells i.e. n-region, p-region and space charge region. Total current produced in the solar cell was calculated by the principle of superposition with the assumption that both sides of the junction is uniformly doped, the values of lifetime remains constant throughout each uniform region, the recombination of excess minority carriers takes place both at the front and the back surface and that "dead layer" exists adjacent to the front surface of the cell. The effects of some parameters affecting on photocurrent will be studied in this chapter. These parameters are junction depth,  $x_j$ , substrate resistivity,  $\rho_p$ , front surface recombination velocity,  $s_p$ , reflection coefficient,  $R$ , surface carrier concentration,  $N_d$  and back surface recombination velocity,  $S_n$

3.2 A study on the Photocurrent in n-Region.

The hole photocurrent in n-region can be determined for low level injection conditions using the continuity equation, at steady state  $\frac{dP_n}{dt} = 0$

$$D_p \frac{d^2 [P_n(x) - P_{no}]}{dx^2} + G(x) - \frac{P_n(x) - P_{no}}{\tau_p} = 0$$

where  $D_p$  is the diffusion coefficient of holes in n-type material.  
( $\text{cm}^2/\text{sec}$ )

$P_n(x)$  is the hole density in n-type material as a function of distance,  $x$  ( $\text{cm}^{-3}$ )

$P_{no}$  is the hole density in equilibrium ( $\text{cm}^{-3}$ )

$G(x)$  is the carrier generation rate due to incident light as a function of distance,  $x$ .

$\tau_p$  is lifetime of holes in n-type material ( $\text{sec}^{-1}$ )

Substituting  $G(x) = \alpha F_0 (1-R) \exp(-\alpha x)$  from Eq.(2) in Eq.(12),

$$\frac{d^2 [P_n(x) - P_{no}]}{dx^2} - \frac{P_n(x) - P_{no}}{L_p^2} = - \frac{\alpha F_0 (1-R) \exp(-\alpha x)}{D_p} \quad (13)$$

The solution of this differential equation is,

$$P_n(x) - P_{no} = A \exp(-x/L_p) - B \exp(x/L_p) - \frac{\alpha F_0 (1-R) \exp(-\alpha x)}{D_p (\alpha^2 - 1/L_p^2)} \quad (14)$$

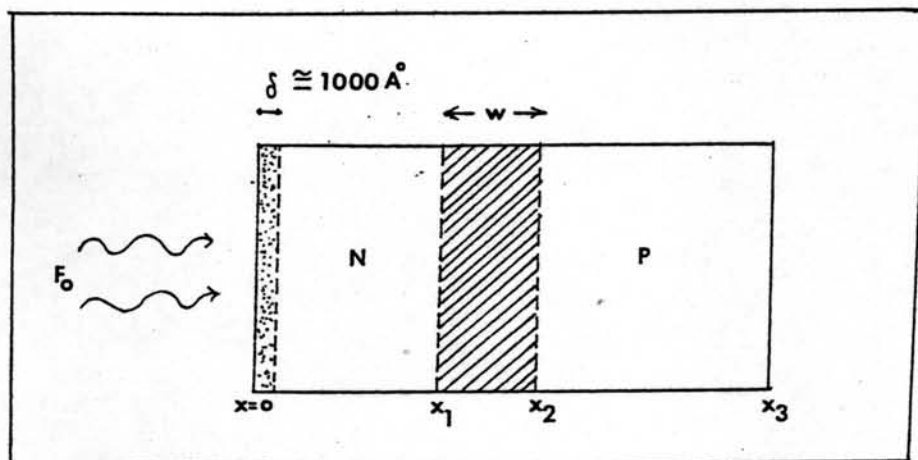


Fig.11 The elaborated model of n-on-p junction solar cell where  $F_0$  represents flux of photons in photons  $\text{cm}^{-2} \text{sec}^{-1}$  per unit band width and  $W$  represents space charge region width and  $\delta$  represents "dead layer".

There are two boundary conditions

1. at the front surface, the recombination take place

$$-D_p \left. \frac{dP_n(x)}{dx} \right|_{x=0} = \alpha F_0 (1-R) [1 - \exp(-\alpha \delta)] - S_p [P_n(x) - P_{no}] \quad (15)$$

where  $\delta$  is the dead layer

$S_p$  is the front surface recombination velocity.

2. while at the junction edge.

$$P_n(x_1) = P_{no} \quad (\text{short-circuit current}) \quad (16)$$

where  $x_1$  is the distance defined in Fig.11

Eq.(15) implies that the recombination rate at the surface is linearly proportional to the concentration of excess minority carriers  $[P_n(x) - P_{no}]$ . The constant in the second term of right-hand-side of Eq.(15) represents the front surface recombination velocity,  $S_p$ , in cm/sec. In addition, the first term of right-hand-side of Eq.(15) results from high front surface concentrations and their associated stress, dislocations and perturbations of the band structure. This leads to a "dead layer",  $\delta$ , of extremely low lifetime over a fraction of the diffused top region adjacent to the surface (around 1 000 Å thick).

Eq. (16) implies that the excess minority carrier density at the junction is equal to zero according to the law of Junction.

By applying boundary conditions both in Equations (16) and (16), the constants A and B in Eq.(14) are found to be

$$A = \frac{\{ \alpha F_0 (1-R) [1 - \exp(-\alpha \delta)] + k (S_p + \alpha D_p) \} \exp(x_1/L_p) - (S_p - D_p/L_p) \exp(-\alpha x_1)}{(S_p + D_p/L_p) \exp(x_1/L_p) - (S_p - D_p/L_p) \exp(-x_1/L_p)}$$

$$B = \frac{(S_p + D_p/L_p) k \exp(-\alpha x_1) - \{ \alpha F_0 (1-R) [1 - \exp(-\alpha \delta)] + k (S_p + \alpha D_p) \} \exp(-x_1/L_p)}{(S_p + D_p/L_p) \exp(x_1/L_p) - (S_p - D_p/L_p) \exp(-x_1/L_p)}$$

Substituting A and B in Eq. (14), the hole density is

$$P_n(x) - P_{no} = A \exp(-x/L_p) + B \exp(x/L_p) - k \exp(-\alpha x) \quad (17)$$

$$\text{where } k = \frac{\alpha F_0 (1-R)}{D_p (\alpha^2 - 1/L_p^2)}$$

Then, the hole photocurrent density at the junction is

$$J_p \Big|_{x=x_1} = -qD_p \frac{dP_n(x)}{dx} \Big|_{x=x_1}$$

$$= qD_p [A/L_p \exp(-x_1/L_p) - B/L_p \exp(x_1/L_p) - \alpha k \exp(-\alpha x_1)] \quad (18)$$

### 3.3 A Study on the Photocurrent in p-Region

Using the equation as in n-region, starting from  $x_2$  of p-region, i.e.  $x_2=0$ , the continuity equation is found to be

$$D_n \frac{d^2}{dx^2} [n_p(x) - n_{po}] + \alpha F_o (1-R) \exp(-\alpha x_2) \exp(-\alpha x) - \frac{n_p(x) - n_{po}}{\tau_n} = 0$$

where  $D_n$  is the diffusion coefficient of electrons in p-type material ( $\text{cm}^2/\text{sec}$ )

$n_p(x)$  is the electron density in p-type material as a function of distance,  $x$ . ( $\text{cm}^{-3}$ )

$n_{po}$  is the electron density in equilibrium. ( $\text{cm}^{-3}$ )

$\tau_n$  is lifetime of holes in p-type material. ( $\text{sec}^{-1}$ )

and  $x_2$  is the distance defined in Fig.11.

By rearranging,

$$\frac{d^2}{dx^2} [n_p(x) - n_{po}] - \frac{n_p(x) - n_{po}}{L_p^2} = \frac{\alpha F_o (1-R) \exp[-(x_2+x)\alpha]}{D_n} \quad (19)$$

The solution of this differential equation is

$$n_p(x) - n_{po} = A \exp(-x/L_n) + B \exp(x/L_n) - \frac{\alpha F_o (1-R)}{D_n} \frac{1}{(\alpha^2 - 1/L_n^2)} \exp[-(x_2+x)\alpha]$$



Two boundary conditions are

$$n_p(0) = n_{p0} \quad (\text{start at point } x=x_2) \quad (20)$$

$$S_n [n_p(x) - n_{p0}] = -D_n \frac{d[n_p(x) - n_{p0}]}{dx} \quad (21)$$

where  $S_n$  is the back surface recombination velocity.

Eq.(20) implies that the excess minority carrier density at the junction is equal to zero according to the law of Junction. Eq.(21) implies that surface recombination takes place at the back surface of the cell.

By applying the above boundary conditions, the electron density in p-region is found to be

$$n_p(x) - n_{p0} = A_1 \exp(-x/L_n) + B_1 \exp(x/L_n) - k_1 \exp[-(x_2+x)\alpha]$$

$$\text{where } k_1 = \frac{\alpha F_0 (1-R)}{D_n} \cdot \frac{1}{(\alpha^2 - 1/L_n^2)}$$

$$A_1 = k_1 \frac{(S_n + D_n/L_n) \exp(-\alpha x_2 + x_3/L_n) - (S_n - \alpha D_n) \exp[-(x_2 + x_3)\alpha]}{(S_n + D_n/L_n) \exp(x_3/L_n) - (S_n - D_n/L_n) \exp(-x_3/L_n)}$$

$$B_1 = k_1 \frac{(S_n - \alpha D_n) \exp[-(x_2 + x_3)\alpha] - (S_n - D_n/L_n) \exp[-\alpha x_2 + x_3/L_n]}{(S_n + D_n/L_n) \exp(x_3/L_n) - (S_n - D_n/L_n) \exp(-x_3/L_n)}$$

Then, the electron photocurrent density in p-region at the junction is

$$J_n = qD_n \left. \frac{dn_p(x)}{dx} \right|_{x=x_2}$$

$$= qD_n k_j \left[ \frac{M}{L_n} \exp(-x_2/L_n) + \frac{N}{L_n} \exp(x_2/L_n) + \alpha \exp(-2x_2\alpha) \right] \quad (22)$$

### 3.4 A Study on the Photocurrent in Space Charge Region.

To consider the photocurrent produces in space-charge region, the assumption is that the electric field is high enough to sweep the excess minority carriers across this region before they can recombine.

The photocurrent produced in space charge region due to the excess minority carriers<sup>(1)</sup> is

$$J_{dr} = q \int_{x_1}^{x_2} \alpha F_0 (1-R) \exp(-\alpha x) dx$$

where  $x_1$  and  $x_2$  are the distances defined in Fig.11

$$\text{Then, } J_{dr} = qF_0 (1-R) \exp(-\alpha x_1) [1 - \exp(-\alpha W)] \quad (23)$$

where  $W$  is the space charge region width which is  $(2\kappa_0 \epsilon_0 V_d / qN_a)^{1/2}$  (24)

$$\text{when } N_d \gg N_a \quad (6)$$

$\kappa_0$  is the dielectric constant of silicon = 11.7

$\epsilon_0$  is the permittivity of free space = 55.4 electronic charge/ $\nu\mu$

$V_d$  is the build-in voltage of p-n junction =  $0.0259 \frac{N_d N_a}{n_i^2}$  volts

### 3.5 Numerical Simulation of n-on-p Silicon Solar Cells.

The photocurrent generated by monochromatic light is given by the sum of Eqs. (18), (22) and (23). Under illumination, the total photocurrent is obtained by integrating all wavelengths of the solar spectrum within the wavelength  $\lambda_g = 1.24/E_g^{(7)}$ .

$$J_{ph} = \int_0^{\lambda_g} [J_p(\lambda) + J_n(\lambda) + J_{dr}(\lambda)] d\lambda \quad (25)$$

A numerical program in FORTRAN IV (see Appendix) is done by integrating all the values of absorption coefficients,  $\alpha$  and the fluxes of photons,  $F_0$  with respect to wavelength.

In the calculation, the following parameters are varied to observe the changing trend of the photocurrent. They are diffusion coefficients,  $D_p$  and  $D_n$ , diffusion lengths,  $L_p$  and  $L_n$  (these values are both dependent on carrier concentrations), front and back surface recombination velocities,  $S_p$  and  $S_n$ , reflectivity,  $R$ , dead layer,  $\delta$ , surface carrier concentration,  $N_d$ , and junction depth,  $x_j$ .

The change of the photocurrent due to each parameter is further discussed in the successive sections. Note that trapezoidal integration technique is used in the numerical integration.

### 3.6 Effects of Variations in Geometrical and Physical Parameters on the Photocurrent.

The assumptions used in simulation are

1. Reflection coefficient is constant at all wavelengths.
2. Solar spectrum is taken at the earth's surface for optimum conditions at sea level, sun at zenith or AML, as shown in Fig.12<sup>(7)</sup> and Table 1



$\lambda$ ( $\mu\text{m}$ )	P.L. $\text{mWcm}^{-2} \mu^{-1}$ (AM1)	P.L. $\frac{\text{photons}}{\text{cm}^2 \text{sec}}$	$\alpha$ ( $\text{cm}^{-1}$ ) (25°C)
0.30	1.00 E 0	1.51 E 15	7.21 E 5
0.32	1.66 E 1	2.67 E 15	4.44 E 5
0.36	4.91 E 1	8.90 E 15	1.62 E 5
0.40	8.73 E 1	1.76 E 16	7.36 E 4
0.44	1.33 E 2	2.95 E 17	3.34 E 4
0.48	1.53 E 2	3.70 E 17	1.89 E 4
0.52	1.53 E 2	4.01 E 17	1.00 E 4
0.56	1.45 E 2	4.09 E 17	6.59 E 3
0.60	1.40 E 2	4.22 E 17	4.25 E 3
0.64	1.30 E 2	4.19 E 17	2.99 E 3
0.68	1.23 E 2	4.21 E 17	2.30 E 3
0.72	1.11 E 2	4.02 E 17	1.62 E 3
0.76	8.58 E 1	3.28 E 17	1.36 E 3
0.80	9.66 E 1	3.89 E 17	1.14 E 3
0.84	9.34 E 1	3.95 E 17	9.16 E 2
0.88	7.62 E 1	3.38 E 17	7.36 E 2
0.92	4.14 E 1	1.92 E 17	5.41 E 2
0.96	6.89 E 1	3.33 E 17	3.81 E 2
1.00	6.89 E 1	3.46 E 17	2.46 E 2
1.04	6.12 E 1	3.20 E 17	1.00 E 2
1.08	5.54 E 1	3.01 E 17	3.00 E 1

Solar spectrum AM1 data

Table 1

3. Absorption coefficient,  $\alpha$ , is as a function of wavelength as shown in Fig. 12 (at 300° K).
4. Diffusion coefficients,  $D_p$  and  $D_n$  and diffusion lengths  $L_p$  and  $L_n$  are functions of doping concentrations as shown in Figures (13) and (14).<sup>(22)</sup>
5. Wavelengths are taken from 0.30  $\mu\text{m}$  to 1.08  $\mu\text{m}$ .
6. Relation between resistivity and carrier concentration for silicon at 300K is shown in Fig. 15<sup>(21)</sup>.

Numerical data for simulation are shown in Table 2

Solar Cell Numerical Parameters for Silicon at 300°K Under AM1 Condition.

n-on-p cells  $N_d = 1 \times 10^{19} \text{ cm}^{-3}$ ,  $D_p = 2.9 \text{ cm}^2/\text{sec}$ ,  $L_p = 3(\times 10^{-4} \text{ cm})$ ,  $\tau_p = 3.1 \times 10^{-8} \text{ sec}$

base ( $\Omega\text{-cm}$ )	$N_a$ ( $\text{cm}^{-3}$ )	$D_n$ ( $\text{cm}^2/\text{sec}$ )	$L_n$ ( $\times 10^{-4} \text{ cm}$ )	$\tau_n$ (sec)	W(no bias) ( $\times 10^{-4} \text{ cm}$ )	$V_d$ (Volts)
20	$6.5 \times 10^{14}$	37	240	$15.5 \times 10^{-6}$	1.26	0.804
10	$1.4 \times 10^{15}$	36	230	$14.6 \times 10^{-6}$	0.87	0.824
5	$2.5 \times 10^{15}$	34	216	$13.7 \times 10^{-6}$	0.66	0.839
1	$1.5 \times 10^{17}$	27	164	$9.9 \times 10^{-6}$	0.28	0.886
0.1	$5.0 \times 10^{17}$	11	52	$2.4 \times 10^{-6}$	0.05	0.976

$\delta = 1000 \text{ \AA}$

Table 2

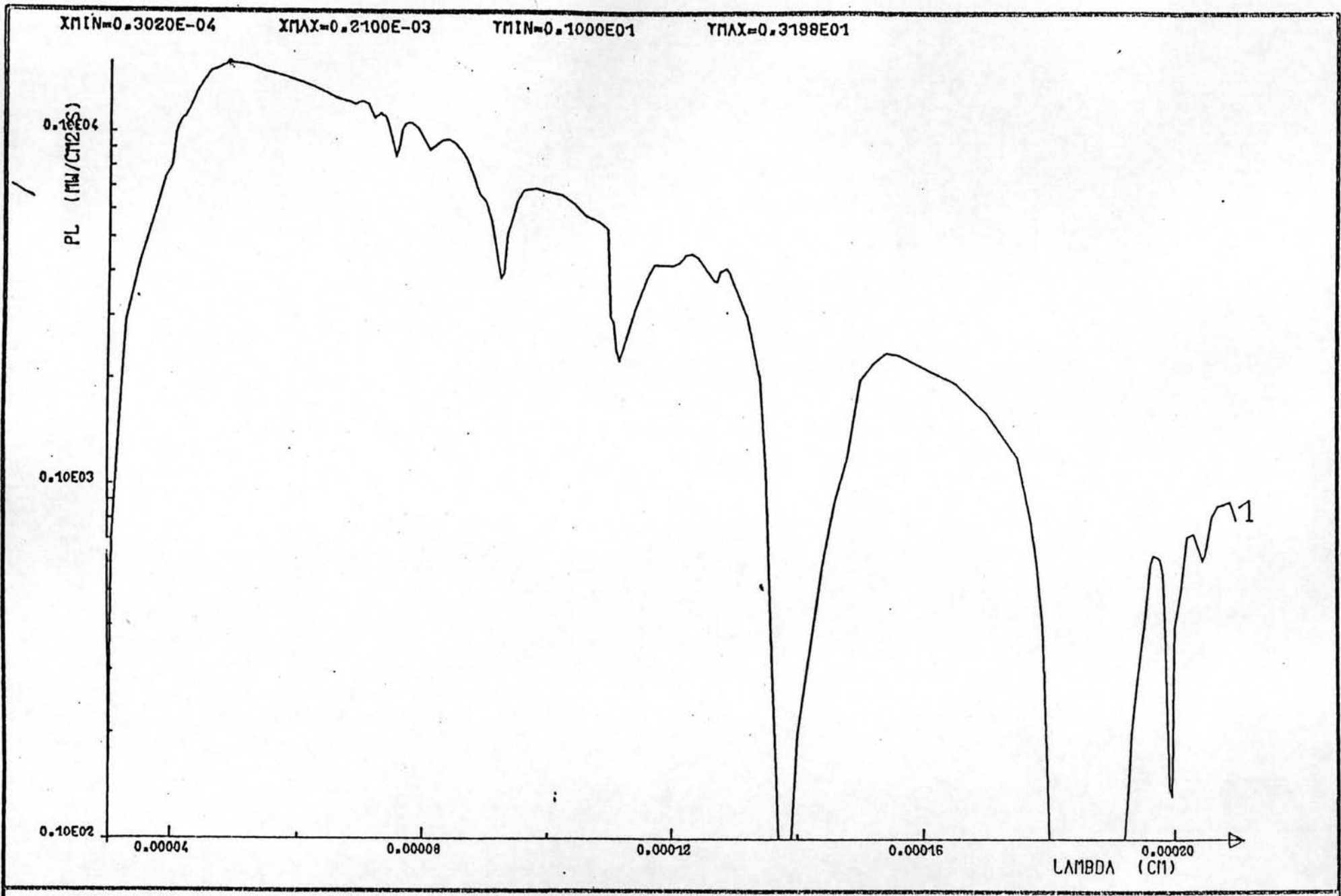


Fig. 12 Solar spectrum, AM1<sup>(7)</sup>

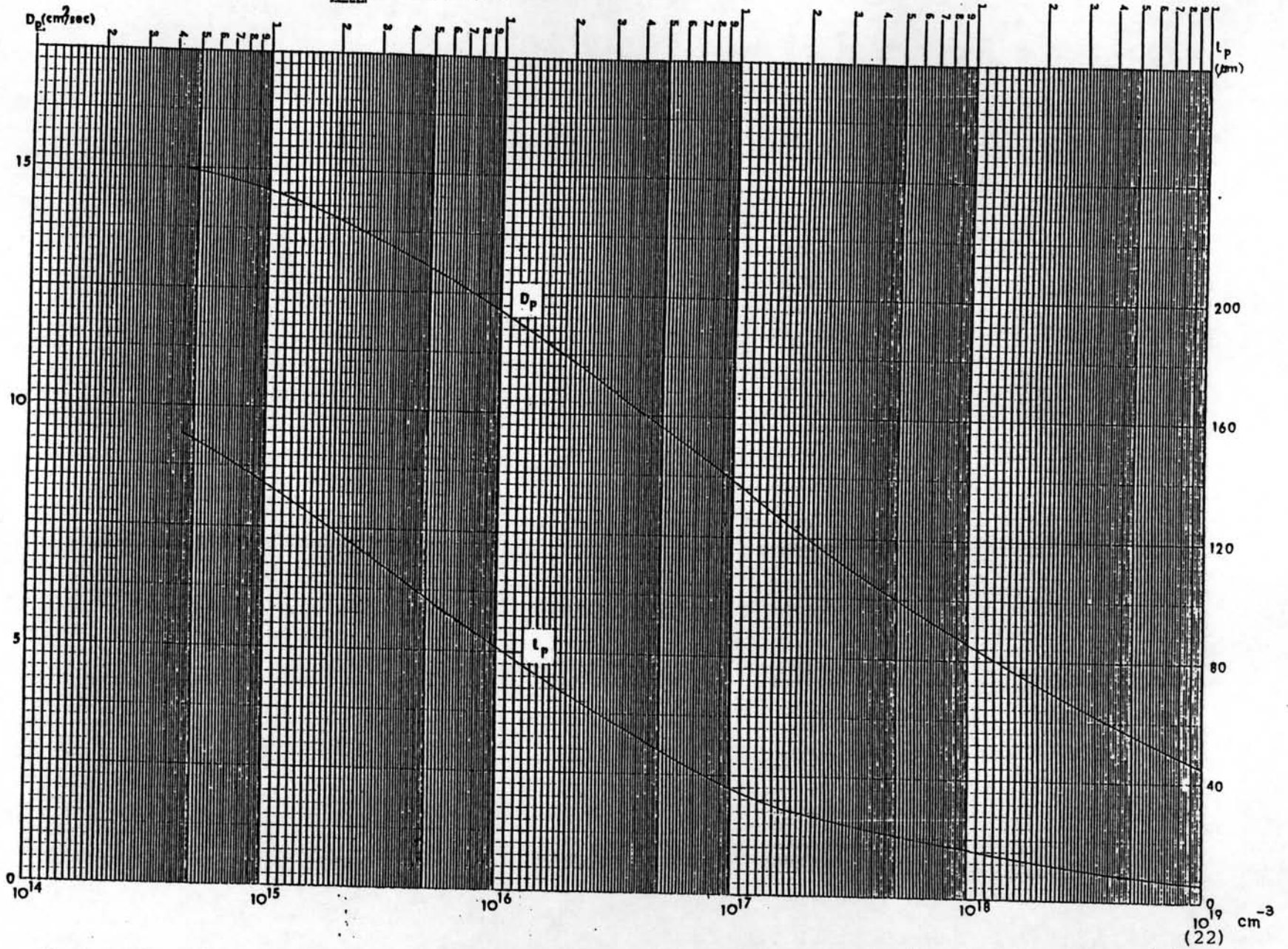


Fig.13 Diffusion coefficient and diffusion length VS. carrier concentration for n-type material.

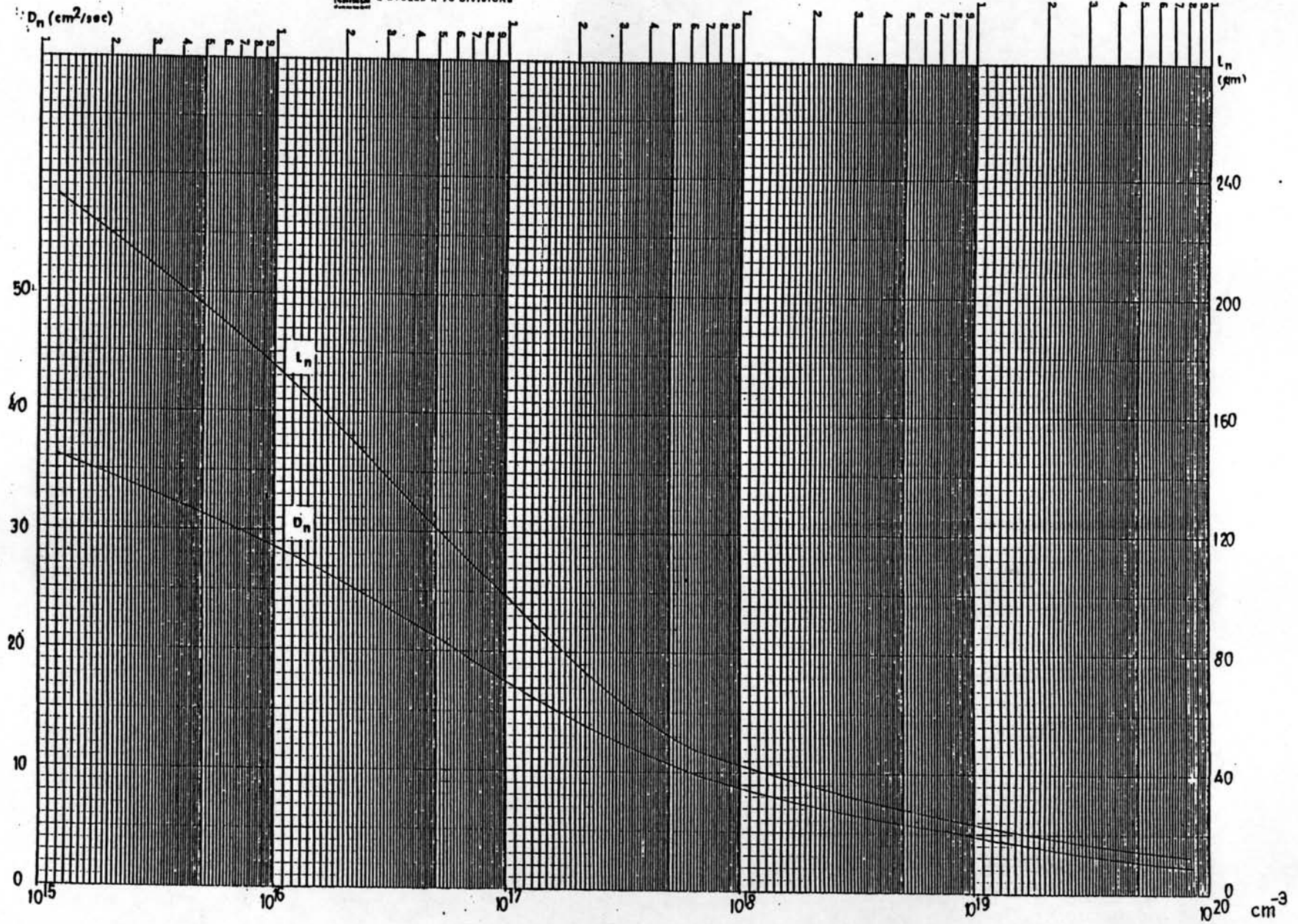


Fig.14 Diffusion coefficient and diffusion length VS. carrier concentration for p-type material

(22)

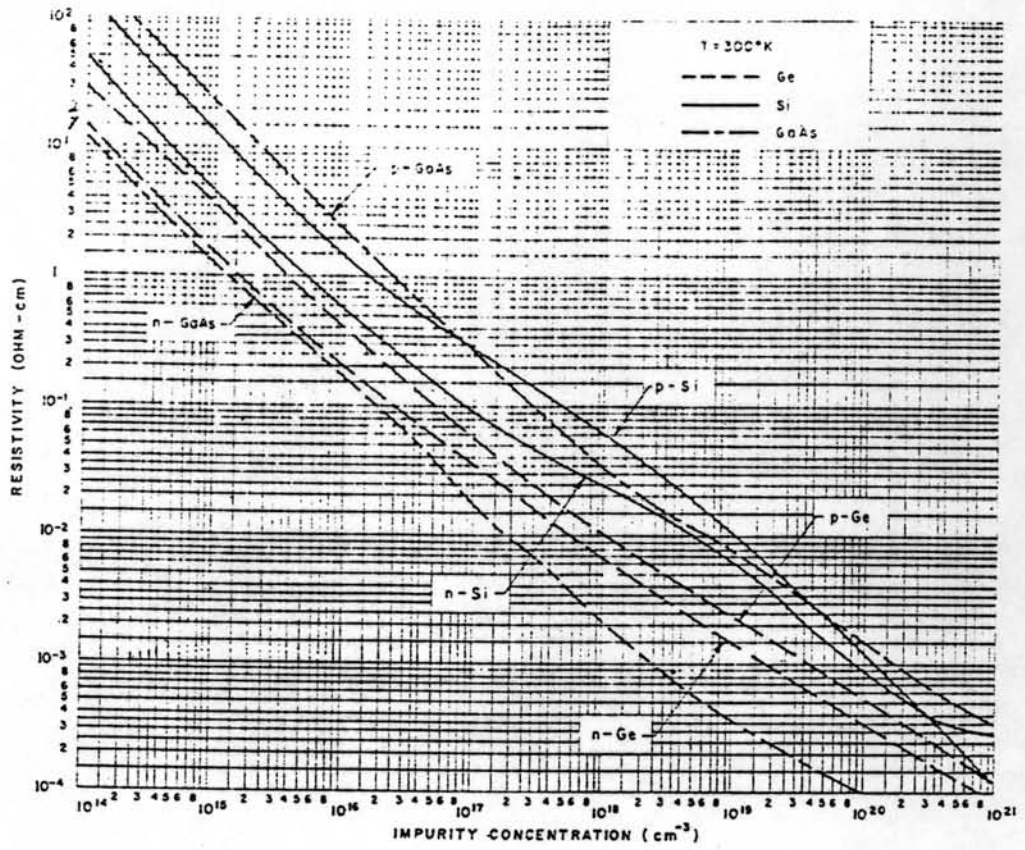


Fig.15 Relationship between resistivity and carrier concentration<sup>(21)</sup>

### 3.6.1 The Effect of Junction Depth, $x_j$ , on the photocurrent.

The calculated results of photocurrents as a function of junction depth is shown in Fig.16.

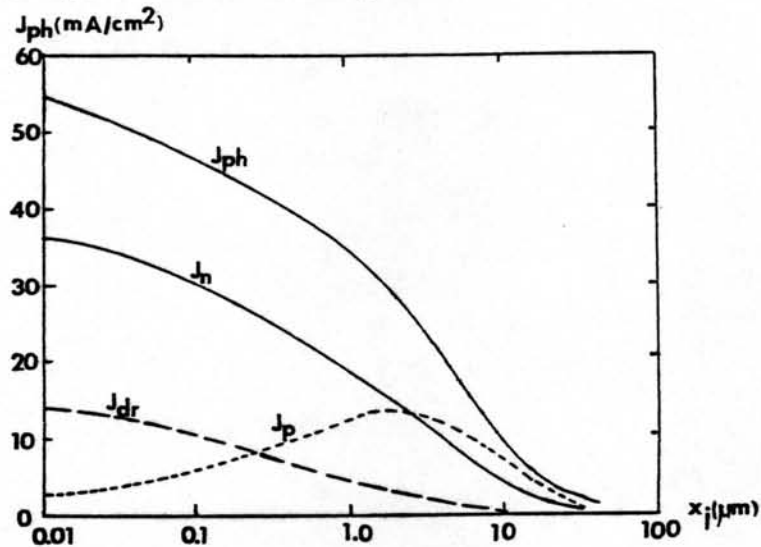


Fig.16 Calculated AM1 photocurrent densities as a function of junction depth. Dead layer has been assumed for the top region. ( $\delta = 1000\text{\AA}$ ) Resistivity and thickness of the n-on-p silicon solar cell are  $10\ \text{cm}$  and  $200\ \mu\text{m}$  respectively front and back surface recombination velocities are  $10^4$  and  $10^6\ \text{cm}/\text{sec}$  respectively. Surface reflectivity of the cell is zero.

The curve shows that the hole photocurrent density,  $J_p$  in n-region is small at the shallow junction depth. This is due to the recombination that takes place at the top surface. The photocurrent,  $J_p$  tends to increase and reaches the maximum value at an arbitrary junction depth. Then, it decays exponentially at deeper junction depth. The photocurrents produced in p-region and space charge region decay exponentially with deeper junction depth. By the superposition principle, the three region photocurrents are summed up to produce the total current in the solar cell. The total

photocurrent decays exponentially with distance because the generated excess minority carriers decrease exponentially with distance according to Lambert law. The calculated results are in good agreement with Hovel and Fossum <sup>(1,8)</sup>. Therefore, the junction depth should be the shallowest in order to yield the highest photocurrent. In fact, shallow junction depth contributes a large series resistance. Then, the junction depth should be optimized at an arbitrary distance.

### 3.6.2 The Effect of Front Surface Recombination Velocity, $S_p$ on the Photocurrent.

The calculated results of photocurrent as a function of junction depth with different front surface recombination velocities,  $S_p$  are shown in Fig. 17.

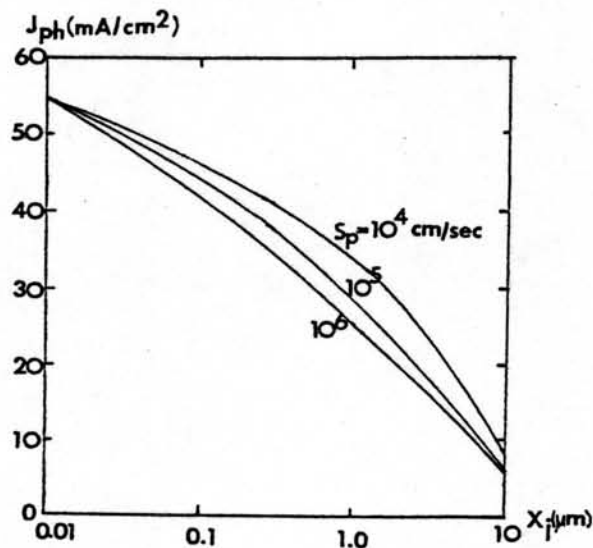


Fig.17 Calculated AM1 photocurrent densities as a function of  $x_j$  with different  $S_p$ . Resistivity of the n-on-p silicon solar cell is  $10 \Omega\text{-cm}$  and  $200 \mu\text{m}$  thick. Back surface recombination velocity is  $10^6 \text{ cm/sec}$  and surface reflectivity of the cell is zero.

The above curve shows that the higher front surface recombination



velocities result in the lower photocurrent. The high front surface recombination velocity due to the surface state causes lower number of collected carriers near the top surface of the cell resulting a lower photocurrent. In general, the front surface recombination velocity is around  $10^5 - 10^6$  cm/sec.<sup>(1)</sup> It can be reduced by decreasing the junction depth, by providing an aiding drift field in the top region and by making a good preparation and polishing of semiconductors wafers.<sup>(1)</sup> For  $S_p$  values of  $10^3$  cm/sec or below, all of the computer calculations have so far indicated an almost completely negligible effect of surface recombination on silicon solar cell properties.<sup>(9)</sup>

To study the effect of dead layer on the photocurrent, the following expression is used.

$$S_p = \sigma_p v_{th} N_t \delta \quad (25)$$

where  $\sigma_p$  is the capture cross sections.

$v_{th}$  is the thermal velocity.

$N_t$  is the recombination center densities.

and  $\delta$  is the dead layer thickness.

The calculated photocurrents as a function of junction depth with different thicknesses of dead layer, are shown in Fig.18.

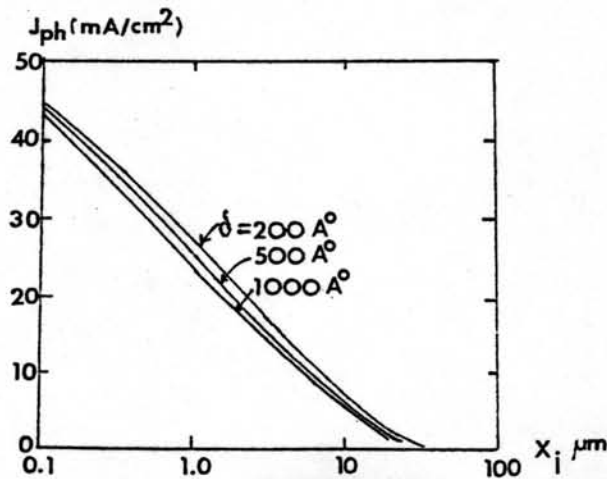


Fig.18 Calculated AM1 photocurrent densities as a function of  $x_j$  with different thicknesses of dead layer. Resistivity of n-on-p silicon solar cell is  $10 \Omega\text{-cm}$  and  $200 \mu\text{m}$  thickness. Front and back surface recombination velocities are  $10^4 \text{ cm/sec}$  and  $10^6 \text{ cm/sec}$  respectively. Surface reflectivity of the cell is zero.

From Fig. 18 it shows that for increasing values of dead layer the photocurrent decreases because of the extremely short lifetime in this region. Dead layer can be decreased by lowering the surface carriers concentration of the diffused region, by reducing the junction depth and by making a good process for surface preparation of wafers<sup>(1,10)</sup>

Fig.18 shows typical phosphorous distributions for junction depths of  $4000 \text{ \AA}$ ,  $2900 \text{ \AA}$  and  $1200 \text{ \AA}$ . It can be seen that the  $4000 \text{ \AA}$  diffusion shows wider dead layer. The layer is measured to be about  $1500 \text{ \AA}$ . However this layer reduces as the junction depth decreases. Schockley has shown that dislocation is not only dependent on surface concentration, but also affected by the total number of impurities (N) found in the surface area<sup>(11)</sup>.

As shown in Fig.19, at different surface concentrations, there are different dead layers which correspond to the total number of surface impurities. Hence, dislocation density is less at the lower surface concentration and at shallower junction depths.

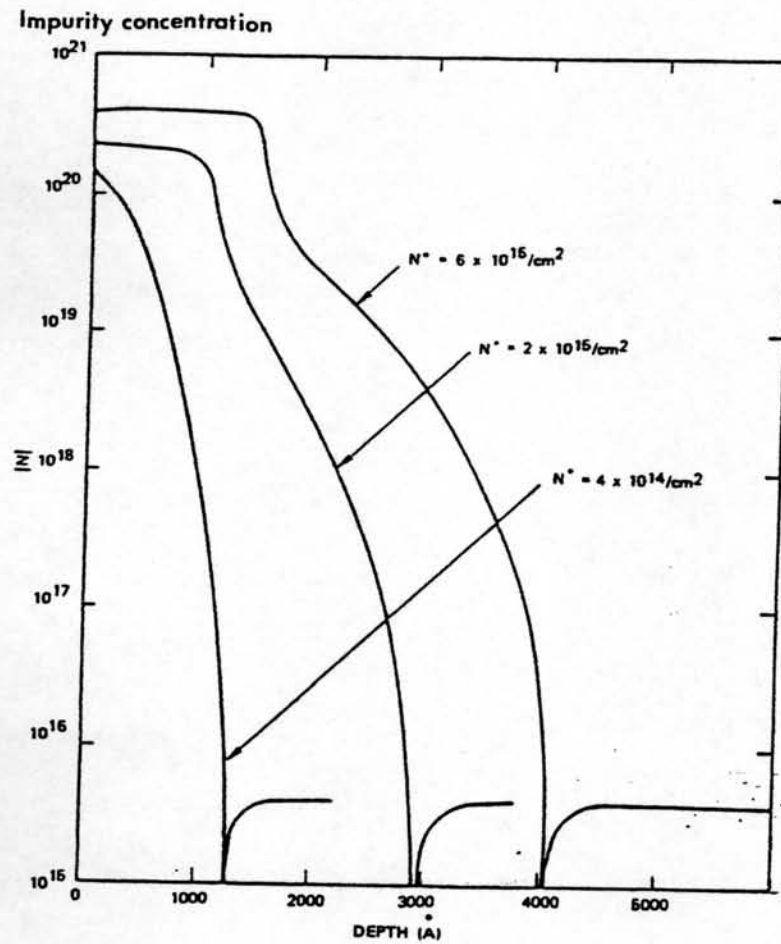


Fig. 19 Diffusion Profiles for Phosphorus in Silicon for  
 Three Junction Depths ( $N^*$  Denotes the Integrated Impurity Concentration). (16)

### 3.6.3 The Effect of Substrate Resistivity, $\rho_b$ , on the Photocurrent

The calculated results of photocurrents as a function of substrate resistivity. With different front surface recombination velocities,  $S_p$  are shown in Fig.20.

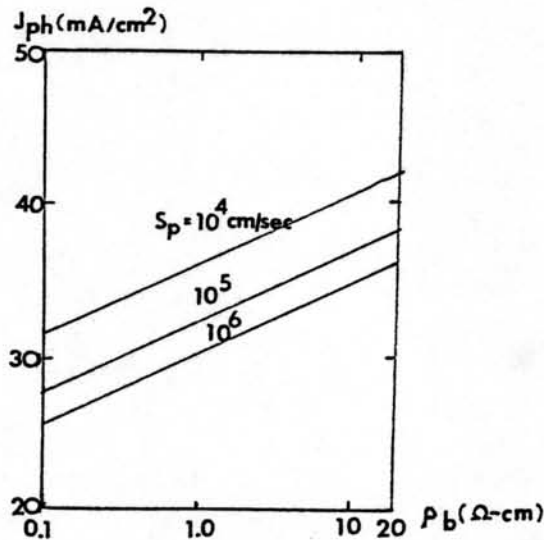


Fig. 20 Calculated AM1 photocurrent densities as a function of  $\rho_b$  with different  $S_p$  at  $x_j = 0.4 \mu\text{m}$ . Resistivity of n-on-p silicon solar cell is  $10 \Omega\text{-cm}$  and  $200 \mu\text{m}$  thick. Back surface recombination velocity of the cell is  $10^6 \text{ cm/sec}$  and surface reflectivity of zero.

The curve of Fig.20 shows that at high substrate resistivities the increase in photocurrent is due to their higher lifetime. As can be seen in Figs. 21 and 22 that lifetime is a function of resistivity. (12)

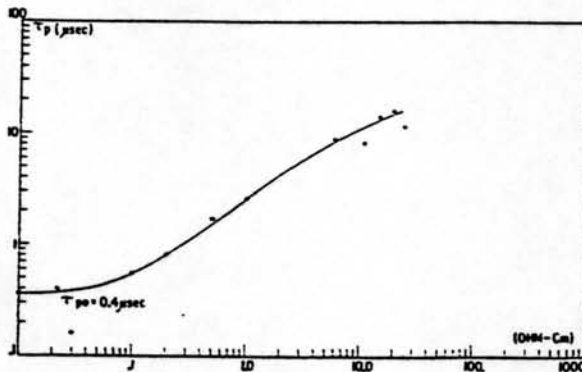


Fig. 21 Lifetime versus resistivity, n-type silicon<sup>(12)</sup>

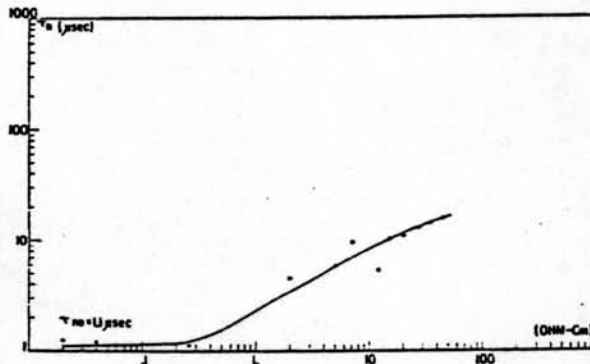


Fig. 22 Lifetime versus resistivity, p-type silicon.<sup>(12)</sup>

On the other hand, the lifetime of the minority carriers (and also the diffusion coefficient and diffusion length) is a strong function of doping concentration as also can be seen in Figures 13 and 14 used in the computations. Hence, photocurrent can be increased by choosing a higher substrate resistivity. However, a high substrate resistivity can cause a reduction in open-circuit voltage as will be shown in the next chapter. An optimum substrate resistivity should be chosen in order to obtain a

high solar cell performance.

### 3.6.4 The Effect of Reflection Coefficient on the Photocurrent.

The calculated results of photocurrents as a function of junction depth with different reflection coefficients are shown in Fig.23.

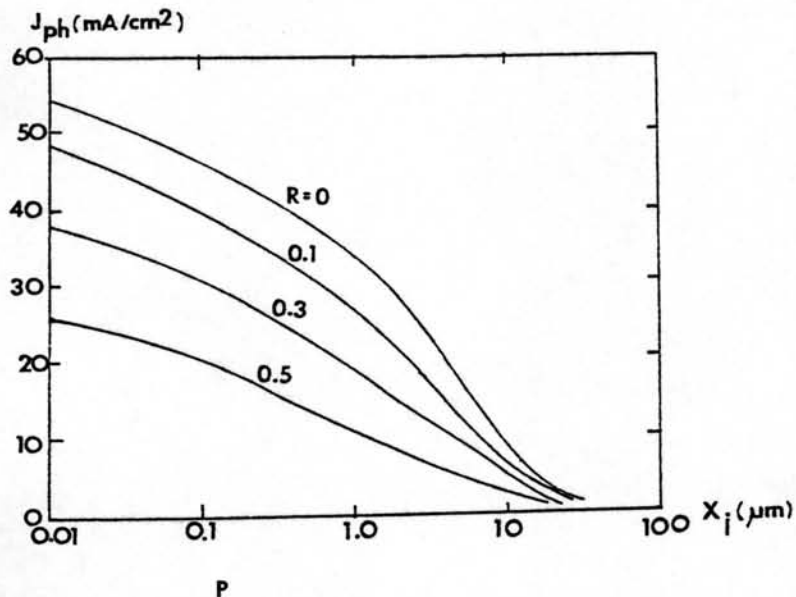


Fig. 23 Calculated AM1 photocurrent densities as a function of  $x_j$  with different reflectivities. Resistivity of n-on-p silicon solar cell is 10 ohm-cm and 200  $\mu\text{m}$  thick. Front and back surface recombination velocities are  $10^4$  cm/sec and  $10^6$  cm/sec respectively.

The curve of Fig.23 shows that at high reflectivities a sharp decrease in photocurrent is due to the reflection of incident photons at the surface of the cell. A major increase in photocurrent can be achieved through antireflection coating layers. For many years SiO and SiO<sub>2</sub> represented the standard antireflection films. Table 3 shows calculated data for several antireflection coating layers by Hauser and Dunbar<sup>(9)</sup>. The surface reflection losses of SiO and SiO<sub>2</sub> are 10.4 and

14.5 percent respectively at AM2. It can be seen that SiO shows a larger generation rate than SiO<sub>2</sub>. However, Ta<sub>2</sub>O<sub>5</sub> shows a better solar cell performance to be an antireflection film. It reduces the surface loss to 9.5 percent at AM2.

The reflectivity of bare Si is reduced from around 35 to 45 percent for flat surface to around 20 percent for the texturized surface, and the addition of an antireflection coating reduces the overall reflection loss to a few percent<sup>(1)</sup>. A double layer coating which is the system consisting of about 600 Å of TiO<sub>2</sub> and 1050 - 1100 Å of SiO<sub>2</sub> or MgF<sub>2</sub> can reduce the reflection loss to 3 percent on the average<sup>(1)</sup>.

Summary of Excess Carrier Generation in Silicon<sup>(9)</sup>

Geometry	Spectral Conditions	Optimum Antireflection Thickness (Å)	Surface Loss (%)	Available (a) photocurrent (mA/cm <sup>2</sup> )	Surface Generation Rate (cm <sup>-3</sup> /sec)
Si	AM0	N <sub>C</sub>	36.4	34.2	1.15x10 <sup>20</sup>
	AM2	N <sub>C</sub>	34.7	22.4	1.62x10 <sup>21</sup>
Si+SiC	AM0	800	15.6	45.4	5.96x10 <sup>21</sup>
	AM2	800	10.4	30.7	1.39x10 <sup>21</sup>
Si+SiO <sub>2</sub>	AM0	1100	17.6	44.3	1.25x10 <sup>22</sup>
	AM2	1100	14.5	29.3	1.83x10 <sup>21</sup>
Ta <sub>2</sub> O <sub>5</sub>	AM0	720	12.5	47.0	1.56x10 <sup>22</sup>
	AM2	720	9.5	31.1	1.89x10 <sup>21</sup>

(a) indicates computed at optimum antireflection thickness if applicable

Table 3

### 3.6.5 The Effect of Solar Cell Thickness on the Photocurrent.

The calculated results of photocurrents as a function of junction depth with different thicknesses are shown in Fig.24.

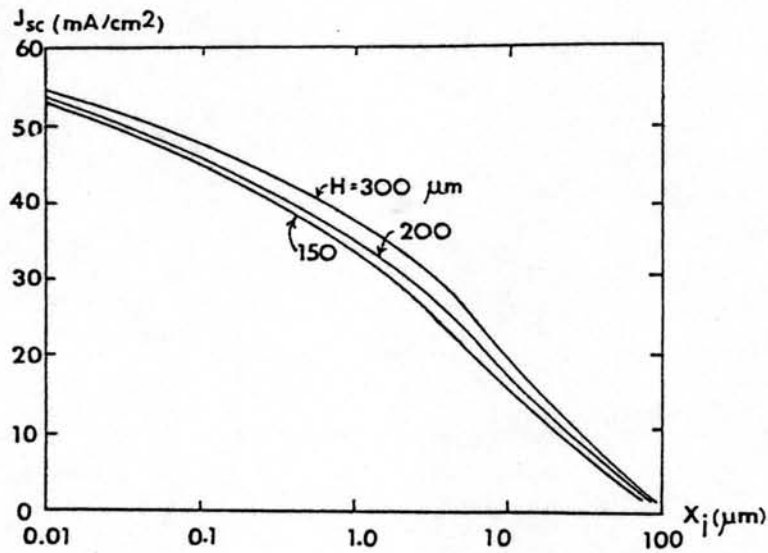


Fig.24 Calculated AM1 photocurrent densities as a function of junction depth with different solar cell thicknesses,  $H$ . The base resistivity of n-on-p silicon solar cell is 10 ohm-cm and surface reflectivity is zero. Front and back surface recombination velocities are  $10^4$  and  $10^6$  cm/sec. respectively.

The curve of Fig.24 shows that by a reduction in the device thickness the photocurrent density tends to decrease because of a reduced collection efficiency. The influence of back contact becomes greater when the solar cell is made thinner than the minority carrier diffusion length in base as can be seen in Table 4. The 20  $\Omega$ -cm (of 240  $\mu\text{m}$  diffusion length) n-on-p silicon solar cells with the thicknesses of 150 and 300  $\mu\text{m}$  show the 0.4  $\mu\text{m}$  junction depth photocurrents at various back surface recombination velocities.



Solar Cell Thickness ( $\mu\text{m}$ )	Back Surface Recombination Velocity (cm/sec)	Photocurrent densities ( $\text{mA}/\text{cm}^2$ )			
		1sun	10suns	50suns	100suns
150	$10^2$	39.84	398.4	1992	3984
	$10^4$	39.20	392.0	1960	3920
	$10^7$	39.07	390.7	1953	3907
300	$10^2$	41.09	410.9	2054	4109
	$10^4$	40.46	404.6	2023	4046
	$10^7$	40.33	403.3	2016	4033

The Effect of Back Surface Recombination Velocities on n-on-p Silicon Solar Cells.

Table 4

### 3.6.6 The Effect of Surface Carrier Concentration on the Photocurrent.

The calculated results of photocurrents as a function of junction depth with different surface carrier concentrations are shown in Fig.25

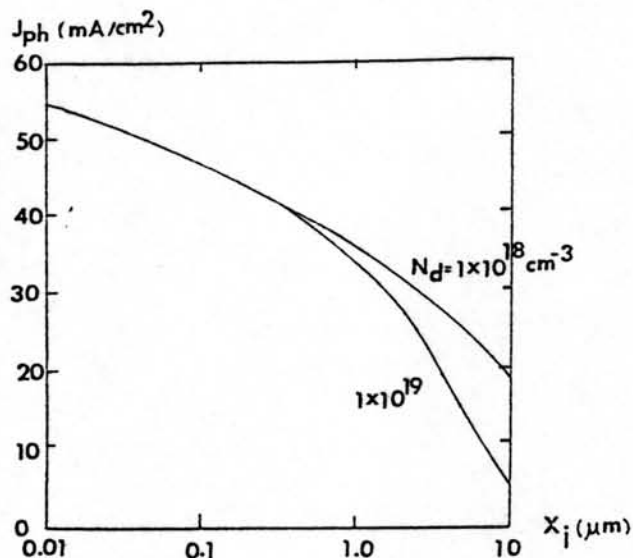


Fig.25 Calculated AM1 photocurrent densities as a function of  $x_j$  with different surface carrier concentrations,  $N_d$ . Resistivity of the n-on-p silicon solar cell is 10 ohm-cm and 200 μm thickness. Front and back surface recombination velocities are  $10^4$  and  $10^6$  cm/sec respectively. Surface reflectivity of the cell is zero.

The curve of Fig.25 shows that the decrease in surface carrier concentration results in a higher photocurrent. The reason is that the high surface carrier concentrations cause the wider dead layers resulting in a lower photocurrent as can be seen in Fig.18 of section 3.6.2.